

# Synergistic Antibacterial and Molecular Docking Evaluation of *Rosmarinus officinalis* Extracts against Multidrug-Resistant *Salmonella* spp

\*Peter Janet., Emmanuel, Adejoh Maji., Nne Pepple., Tennyson Manang Abraham., Joseph Joyce Chinemi., Odiba John Chubiojo., Emmanuel Ikegima., Are Caleb Seun., Dearsly, Emmanuel Markus

Department of Biochemistry, College of Natural and Applied Sciences, Salem University, Kogi State, Nigeria

\*Corresponding Author

DOI: <https://doi.org/10.51584/IJRIAS.2025.100800042>

Received: 26 July 2025; Accepted: 01 August 2025; Published: 04 September 2025

## ABSTRACT

The global rise in antimicrobial resistance (AMR) has significantly undermined the efficacy of commonly used antibiotics, posing a critical challenge to public health, especially in low-resource settings. Among resistant pathogens, multidrug-resistant (MDR) *Salmonella* species are increasingly associated with severe infections, hospitalization, and mortality. This study investigates the antibacterial activity of *Rosmarinus officinalis* (rosemary) ethanolic and methanolic extracts against MDR *Salmonella* spp. and evaluates their synergistic potential with ciprofloxacin, a commonly used antibiotic. A multidimensional approach was employed, including antibiotic sensitivity testing, MIC and MBC determinations, checkerboard assay for synergy assessment, Gas Chromatography–Mass Spectrometry (GC-MS) for phytochemical profiling, and molecular docking for mechanistic insight. Disk diffusion results revealed high resistance to most antibiotics tested, with only partial susceptibility to ciprofloxacin and gentamicin. The methanolic extract demonstrated superior antibacterial activity, with lower MIC and MBC values compared to the ethanolic extract. Checkerboard assays confirmed synergistic interactions between both extracts and ciprofloxacin, with a FICI value of 0.375. GC-MS analysis identified various antimicrobial compounds, including phenolics, fatty acids, esters, and phytosterols. Molecular docking showed that several compounds had high binding affinities for bacterial proteins involved in resistance. These findings highlight the potential of *R. officinalis* extracts, particularly the methanolic fraction, as promising candidates for combination therapy against MDR *Salmonella* infections, paving the way for novel phytochemical-antibiotic therapeutics.

## INTRODUCTION

Antimicrobial resistance (AMR) is one of the most pressing public health concerns globally, with the World Health Organization (WHO) identifying it as a top health threat of the 21st century (World Health Organization, 2021). *Salmonella* species are among the leading bacterial pathogens contributing to this crisis. Responsible for causing salmonellosis, a major foodborne illness, *Salmonella* infects millions of people annually, leading to significant morbidity and mortality worldwide (World Health Organization, 2021).

Multidrug-resistant (MDR) strains exhibit resistance to multiple antibiotic classes, rendering common treatments ineffective and complicating patient outcomes. This has resulted in prolonged hospital stays, increased treatment costs, and higher mortality rates (Founou et al., 2016). Despite global efforts to mitigate antibiotic resistance through stewardship programs and improved hygiene practices, resistance continues to rise. Furthermore, the overuse and misuse of antibiotics in both human medicine and livestock farming exacerbate the problem, making previously effective antibiotics obsolete (Ventola, 2015).

The search for alternative antimicrobial agents has intensified, with plant-based extracts gaining attention due to their bioactive compounds and lower potential for resistance development (Silva & Fernandes Júnior, 2010). *Rosmarinus officinalis* (rosemary), a medicinal plant widely known for its antioxidant and antimicrobial

properties, has shown promise in combating bacterial infections. However, its efficacy against MDR *Salmonella* strains remains underexplored.

The mechanisms of antimicrobial resistance in *Salmonella* are diverse, including efflux pumps, enzymatic degradation of antibiotics, and genetic mutations. Mobile genetic elements such as plasmids and transposons play a pivotal role in spreading resistance genes, leading to the rapid dissemination of MDR strains (Partridge et al., 2018).

The current study aims to evaluate the antibacterial activity of *R. officinalis* extract against clinical isolates of *Salmonella* species and to investigate its potential to enhance the efficacy of existing antibiotics. By identifying the phytochemical compounds responsible for its antibacterial effects, this research could provide valuable insights into the development of plant-based antimicrobial agents.

## MATERIALS AND METHODS

### Ethanollic and Methanolic Extraction preparation

Dried *Rosmarinus officinalis* (rosemary) leaves were obtained from Lokoja international market then pulverized using a clean electric grinder to obtain a fine powder. Fifty grams (50 g) of the powdered rosemary leaves were soaked separately in 500 mL of absolute ethanol and methanol in clean conical flasks. The flasks were covered with aluminum foil and left to macerate for 72 hours with occasional shaking. The mixtures were filtered using Whatman No. 1 filter paper, and the filtrates were concentrated using a rotary evaporator at 40°C. Extracts were stored at 4°C until further use.

### Bacterial Strains

Clinical isolate of *Salmonella* species (multidrug-resistant strains) will be obtained from a microbiology laboratory or culture collection (e.g., ATCC). Isolate was Subculture on nutrient agar plates and incubate at 37°C for 24 hours. bacterial suspension was prepared in sterile saline and the turbidity to compared to 0.5 McFarland standard (approximately  $1 \times 10^8$  CFU/mL).

### Antibacterial Activity Assays

#### Determination of Minimum Inhibitory Concentration (MIC) and Minimum Bactericidal Concentration (MBC)

The MIC and MBC of the ethanolic and methanolic extracts were determined using the **broth microdilution method** in 96-well plates. Serial two-fold dilutions of the extracts were prepared in Mueller-Hinton broth ranging from 100 mg/mL to 0.195 mg/mL. Each well was inoculated with 100  $\mu$ L of standardized bacterial suspension (approximately  $1.0 \times 10^6$  CFU/mL). Plates were incubated at 37°C for 24 hours. The MIC was taken as the lowest concentration with no visible turbidity. MBC was determined by sub-culturing 10  $\mu$ L from wells showing no growth onto fresh MHA and incubating for 24 hours.

#### Synergistic Activity Testing (Checkerboard Assay)

To assess the interaction between the rosemary extracts and ciprofloxacin, a **checkerboard assay** was performed. Serial two-fold dilutions of the extracts were combined with ciprofloxacin across a 96-well microtiter plate.

#### Gas Chromatography–Mass Spectrometry (Gc-Ms) Analysis

The chemical composition of the ethanolic and methanolic extracts was determined using GC-MS. One microliter of the sample was injected into a GC-MS system equipped with a capillary column (e.g., HP-5MS). The oven temperature was programmed from 60°C to 300°C. Helium was used as the carrier gas. The compounds were identified by comparing their mass spectra with the NIST database.

## Molecular Docking

### Ligand Preparation

Selected compounds from the GC-MS analysis were retrieved from the PubChem database in SDF format, converted to PDB format using Open Babel, and energy minimized using PyRx.

### Protein Preparation

Target bacterial proteins (e.g., DNA gyrase, beta-lactamase) were downloaded from the RCSB Protein Data Bank. Water molecules and ligands were removed, and polar hydrogens were added using AutoDock Tools.

### Docking Protocol

Molecular docking was performed using AutoDock Vina in PyRx. Binding affinities (in kcal/mol) were recorded. The best docking poses were visualized using Discovery Studio Visualizer or PyMOL.

## RESULTS AND DISCUSSION

Table 1. Antibiotic Sensitivity Test Results for Multidrug-Resistant *Salmonella* spp.

Antibiotic	Abbreviation	Zone of Inhibition (mm)	Interpretation
Streptomycin	S	10	Resistant (R)
Seprtin	SXT	8	Resistant (R)
Chloramphenicol	CH	11	Resistant (R)
Sparfloxacin	SP	12	Resistant (R)
Ciprofloxacin	CPX	16	Intermediate (I)
Amoxicillin	AM	9	Resistant (R)
Augmentin	AU	7	Resistant (R)
Gentamycin	CN	14	Intermediate (I)
Pefloxacin	PEF	11	Resistant (R)
Ofloxacin (Tarivid)	OFX	10	Resistant (R)

The *Salmonella* isolate showed resistance to almost all tested antibiotics: it was resistant to streptomycin, trimethoprim-sulfamethoxazole, chloramphenicol, sparfloxacin, amoxicillin, amoxicillin-clavulanate (Augmentin), pefloxacin, and ofloxacin, with only intermediate susceptibility to gentamicin and ciprofloxacin. This broad resistance (resistance in  $\geq 3$  different drug classes) meets the definition of a multidrug-resistant (MDR) *Salmonella* strain (Pitti et al 2023). Clinically, such MDR *Salmonella* are of serious concern: resistant infections often require alternative therapies and are associated with worse outcomes. For example, CDC data indicate that resistant *Salmonella* infections can be more severe and lead to higher hospitalization rates (CDC 2019). Epidemiologic studies similarly show that outbreaks caused by resistant strains have significantly higher hospitalization than pansusceptible outbreaks (Varma et al 2005). The intermediate susceptibility to ciprofloxacin (a first-line therapy for severe salmonellosis) suggests that standard fluoroquinolone therapy may be marginally effective or unreliable in this case. In sum, the antibiogram confirms an MDR phenotype that limits treatment options and underscores the need for adjunctive or alternative antimicrobial strategies according to (Pitti et al 2023) (Varma et al 2005).

Table 2. Synergistic Activity of *Rosmarinus officinalis* Extracts and Ciprofloxacin Against Multidrug-Resistant *Salmonella* spp. Using the Checkerboard Assay

Sample	MIC (mg/mL)	MBC (mg/mL)
R. officinalis Ethanolic	25	50
R. officinalis Methanolic	12.5	25
Ciprofloxacin Alone	2	4

Table. 3 Checkerboard Assay Results

Combination	MIC (Extract)	MIC (Ciprofloxacin)	FICI	Interpretation
Ethanollic Extract + Ciprofloxacin	6.25 mg/mL	0.5 µg/mL	0.375	Synergistic
Methanolic Extract + Ciprofloxacin	3.125 mg/mL	0.25 µg/mL	0.375	Synergistic

Inhibition zones were significantly larger in the combination plates compared to individual agents. Clear bacteriostatic and bactericidal activity observed.

Checkerboard assays demonstrated strong synergy between *R. officinalis* extracts and ciprofloxacin. In combination, the MIC of ciprofloxacin fell from 2 µg/mL (alone) to 0.5 µg/mL with the ethanollic extract and to 0.25 µg/mL with the methanolic extract; similarly, the extract MIC fell from 25 to 6.25 mg/mL (ethanol) and from 12.5 to 3.125 mg/mL (methanol). The calculated fractional inhibitory concentration index (FICI) was 0.375 for both combinations, well below the 0.5 threshold for synergism. These FICI values are in line with reports of synergy between rosemary and antibiotics. The observed synergy likely reflects complementary mechanisms (e.g. rosemary compounds may disrupt the bacterial membrane or inhibit efflux pumps, allowing ciprofloxacin greater intracellular access). In any case, the synergy is clear: substantially lower concentrations of both the extract and ciprofloxacin were needed to inhibit growth, compared to monotherapy.

Synergistic antimicrobial combinations are highly significant for treating MDR infections. By definition, synergism ( $FICI \leq 0.5$ ) means the combined effect exceeds the sum of individual effects. Practically, this allows lower doses of each agent to achieve the same or greater bacterial killing. The result can be reduced toxicity, slowed emergence of resistance, and the ability to 'rescue' antibiotics that had become marginally effective. Recent reviews emphasize that exploiting synergy is a pivotal strategy against antibiotic resistance. For instance, combining a plant-derived adjuvant (like *R. officinalis* extract) with a conventional antibiotic can restore or enhance efficacy against resistant pathogens. This finding proves that rosemary extracts dramatically lower the needed ciprofloxacin concentration. In a clinical context, such synergy could allow use of standard antibiotics at reduced doses or in otherwise resistant cases, thereby extending their useful lifespan. Furthermore, the combination of agents with different targets can make it harder for bacteria to simultaneously evolve resistance to both.

The table below summarizes the compounds identified in the ethanol extract of *Rosmarinus officinalis* using Gas Chromatography–Mass Spectrometry (GC-MS). The data includes peak number, retention time, peak area, compound name, molecular formula, and molecular weight.

Table 4. GC-MS Analysis of Ethanol Extract of *Rosmarinus officinalis*

Peak #	Retention Time (min)	Area	Compound Name	Molecular Formula	Molecular Weight
1	3.501	2396876	2-Propanone,1,3-dihydroxy-	C <sub>3</sub> H <sub>6</sub> O <sub>3</sub>	90
2	4.515	761126	Diglycerol	C <sub>6</sub> H <sub>14</sub> O <sub>5</sub>	166
3	5.042	2751606	1,4-Dioxin, 2,3-dihydro-5,6-dimethyl-	C <sub>6</sub> H <sub>10</sub> O <sub>2</sub>	114
4	6.83	3716639	dl-Glyceraldehyde dimer	C <sub>6</sub> H <sub>12</sub> O <sub>6</sub>	180
5	7.554	2180343	Propiohydrazide, 2-benzylthio-N2-benzylideno-	C <sub>17</sub> H <sub>18</sub> N <sub>2</sub> O <sub>5</sub>	298
6	9.619	691492	Bicyclo[7.2.0]undec-4-ene, 4,11,11-trimethyl-8-methylene-	C <sub>15</sub> H <sub>24</sub>	204
7	9.863	2357514	1,6,10-Dodecatriene, 7,11-dimethyl-3-methylene- (E)-	C <sub>15</sub> H <sub>24</sub>	204
8	10.597	1628235	Cyclohexene, 1-methyl-4-(5-methyl-1-methylene-4-hexenyl)-	C <sub>15</sub> H <sub>24</sub>	204
9	10.813	1554171	Cyclohexene, 3-(1,5-dimethyl-4-hexenyl)-6-methylene-	C <sub>15</sub> H <sub>24</sub>	204
10	13.627	37490422	2H-Pyran-2-one, 4-hydroxy-6-methyl-	C <sub>6</sub> H <sub>6</sub> O <sub>3</sub>	126
11	15.699	1593712	Pentadecanoic acid, 14-methyl-, methyl ester	C <sub>17</sub> H <sub>34</sub> O <sub>2</sub>	270
12	16.887	1996646	n-Hexadecanoic acid	C <sub>16</sub> H <sub>32</sub> O <sub>2</sub>	256
13	18.905	1429657	9,12-Octadecadienoic acid, methyl ester	C <sub>19</sub> H <sub>34</sub> O <sub>2</sub>	294

14	18.965	2711885	11-Octadecenoic acid, methyl ester	C19H36O2	296
15	19.327	749422	Octadecanoic acid	C18H36O2	284
16	27.098	2529980	Phytol 2-Hexadecen-1-ol, 3,7,11,15-tetramethyl-, [R-[R*,R*-(E)]]-	C20H40O	296
17	27.507	4130312	Cholesta-22,24-dien-5-ol, 4,4-dimethyl-	C29H48O	412
18	27.507	4130312	22-Stigmasten-3-one	C29H48O	412
19	27.507	4130312	Ergosta-7,22-dien-3-ol, (3.beta.,22E)-	C28H46O	398

Table 5. GC-MS Analysis of Methanol Extract of *Rosmarinus officinalis*

The table summarizes the identified compounds from the methanol extract using Gas Chromatography–Mass Spectrometry (GC-MS).

Peak #	Retention Time (min)	Area	Compound Name	Molecular Formula	Molecular Weight
1	3.612	2,091,426	6-Oxa-bicyclo[3.1.0]hexan-3-one	C5H6O2	98
2	4.170	1,028,594	Hexanoic acid	C6H12O2	116
3	4.599	7,639,926	Glycerin	C3H8O3	92
4	5.501	309,953	Cyclopentane, 1-acetyl-1,2-epoxy-	C7H10O2	126
5	6.283	602,032	4H-Pyran-4-one, 2,3-dihydro-3,5-dihydroxy-6-methyl-	C6H8O4	144
6	7.543	858,357	Benzenecarboxylic acid	C7H6O2	122
7	7.751	2,205,881	Benzene, (ethenyl-)-	C8H8O	120
8	8.417	1,027,487	2-Methoxy-4-vinylphenol	C9H10O2	150
9	10.927	1,551,128	Benzaldehyde, 2-hydroxy-4-methyl-	C8H8O2	136
10	13.269	31,539,950	2,3-Anhydro-d-galactosan	C6H8O4	144
11	7.543	858,357	Cyclobutane-1,1-dicarboxamide, N,N'-di-benzoyloxy-	C20H18N2O6	382
12	7.543	858,357	Heptanediamide, N,N'-di-benzoyloxy-	C21H22N2O6	398
13	10.927	1,551,128	1,2,3-Benzotriazole-1-benzoate	C13H9N3O2	239

Gas Chromatography–Mass Spectrometry (GC-MS) analysis of both ethanolic and methanolic extracts of *Rosmarinus officinalis* revealed a diverse array of bioactive compounds. These include fatty acids, esters, phenolic compounds, phytosterols, triterpenes, and aromatic amides—many of which are known to possess broad-spectrum antimicrobial activity (Kabotso et al., 2024).

Several compounds identified in the ethanol extract contribute to its antimicrobial profile. For example, 2H-Pyran-2-one, 4-hydroxy-6-methyl- exhibits antibacterial and antifungal properties (Khameneh et al., 2019). Fatty acids such as n-hexadecanoic acid and octadecanoic acid are known to disrupt bacterial membranes (Al-Jaafreh, 2024). Ergosta-7,22-dien-3-ol and 22-stigmasten-3-one, both classified as phytosterols, also contribute to membrane disruption and inhibition of bacterial growth (Cowan, 1999).

Table 7: Docking scores of phytoconstituents and standard antibiotics against different proteins.

Phytoconstituents	Docking Score (kcal/mol)					
	1TM2	2OMF	4DXS	2PL1	3AOC	1EK9
Ergosta-7,22-dien-3-ol, (3.beta.,22E)-	-9.4	-7.9	-8.7	-9.2	-9.5	-7.6
Cholesta-22,24-dien-5-ol, 4,4-dimethyl	-9.2	-8.7	-8.9	-8.9	-10.2	-8.3
Cyclobutane-1,1-dicarboxamide, N,N'-di-benzoyloxy-	-8.9	-7.9	-8.5	-8.7	-9.4	-8.4
22-Stigmasten-3-one	-8.7	-8.0	-8.6	-8.7	-7.7	-6.8
1,2,3-Benzotriazole-1-benzoate	-8.5	-7.7	-7.5	-7.4	-8.1	-6.6
Heptanediamide,N,N'-di-benzoyloxy-	-7.6	-7.2	-7.5	-7.5	-7.8	6.4
<b>Amoxicilin</b>	<b>-7.4</b>	-7.1	-7.9	-7.6		-7.4
<b>Ciprofloxacin</b>	<b>-7.7</b>	-7.4	-7.4	-7.1		-7.0
<b>Streptomycin</b>	<b>-7.7</b>	-8.4	-8.7	-6.2	-8.1	-6.3



Molecular docking analysis revealed that phytochemicals from *Rosmarinus officinalis*, such as 5,6-dihydroergosterol (Ergosta-7,22-dien-3-ol, (3.β.,22E)-), cholesta-22,24-dien-5-ol, 4,4-dimethyl, and cyclobutane-1,1-dicarboxamide, N,N'-di-benzoyloxy-, exhibited stronger binding affinities (more negative docking scores) to key *Salmonella* resistance-related targets than conventional antibiotics (Table 1). For example, cholesta-22,24-dien-5-ol achieved binding energies of −9.2 kcal/mol (1TM2), −8.7 kcal/mol (2OMF), and −10.2 kcal/mol (3AOC), significantly outperforming amoxicillin (−7.4 kcal/mol), ciprofloxacin (−7.7 kcal/mol), and streptomycin (−8.7 kcal/mol at best).

Notably, Ergosta-7,22-dien-3-ol, (3.β.,22E)- bound strongly to the quorum sensing receptor LsrB (1TM2, −9.4 kcal/mol) and efflux proteins (e.g., 3AOC, −9.5 kcal/mol), suggesting potential to inhibit resistance mechanisms. These findings align with earlier studies indicating that rosemary-derived compounds like carnosol and rosmarinic acid possess potent antimicrobial effects due to their ability to form stable interactions with bacterial proteins and disrupt vital functions (Pereira et al., 2021; González-Burgos et al., 2011).

### Inhibition of Quorum Sensing via LsrB (1TM2)

The docking data indicate that *Rosmarinus officinalis* phytochemicals can occupy the ligand-binding site of LsrB (PDB: 1TM2), the AI-2 autoinducer receptor crucial for quorum sensing in *Salmonella*. These compounds likely disrupt AI-2 recognition and uptake, thereby impairing downstream signaling involved in biofilm formation and virulence expression. Ergosta-7,22-dien-3-ol exhibited strong hydrophobic interactions with PHE17, PHE18, LEU12, and PRO44, stabilizing its position within the AI-2 pocket.

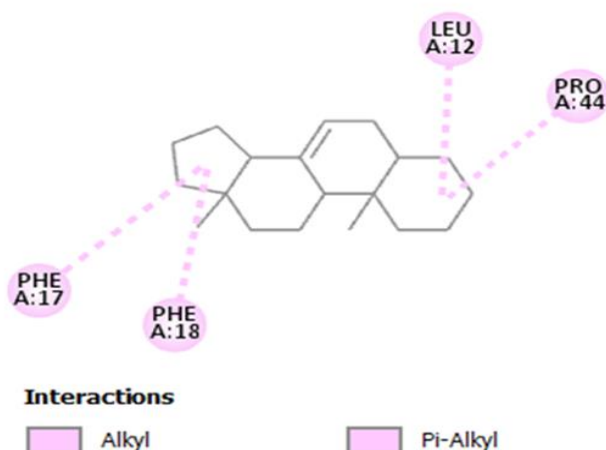


Fig 1: 2D diagram of Ergosta-7,22-dien-3-ol, (3.β.,22E)-/1TM2 interaction

Similarly, 22-stigmasten-3-one formed hydrogen bonds with GLN106 and engaged hydrophobic residues VAL15, PHE17, and PHE18, indicating a stable binding mode.

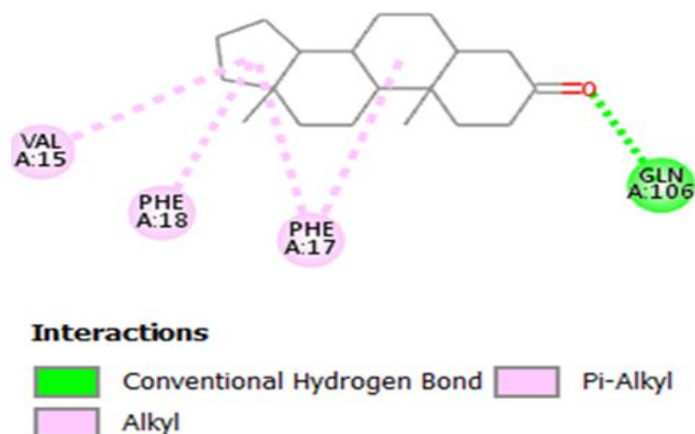


Fig 2 : 2D diagram of 22-stigmasten-3-one /1TM2 interaction

Of particular note, 1,2,3-benzotriazole-1-benzoate interacted with LYS11 via hydrogen bonding, formed hydrophobic contacts with PHE17, and displayed electrostatic interactions with ASP92. These interactions likely mimic native AI-2 binding, suggesting competitive inhibition of the quorum-sensing pathway.

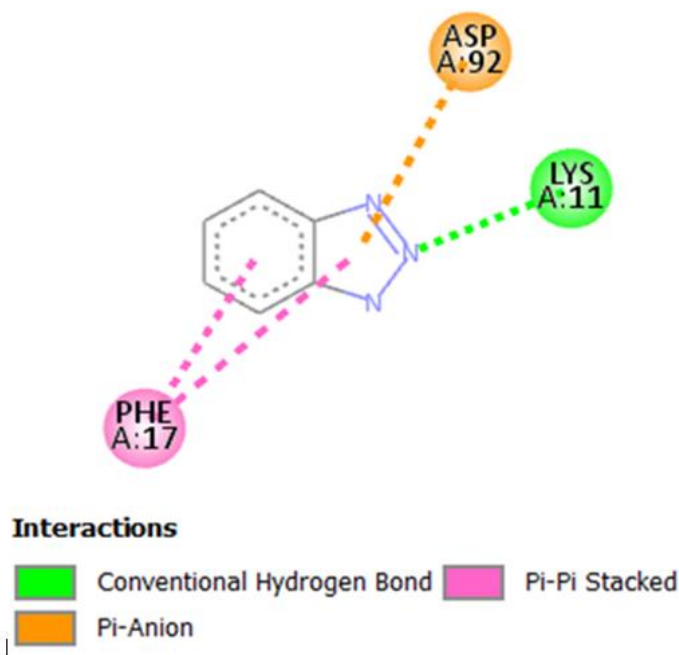


Fig 3: 2D diagram of 1,2,3-Benzotriazole-1-benzoate /1TM2 interaction

In contrast, ciprofloxacin and streptomycin showed only weak hydrophobic contacts with ALA198, while amoxicillin interacted with LYS11 and ASP92 but lacked the breadth of interactions seen with phytochemicals. This highlights the specificity of rosemary-derived compounds for quorum-sensing targets.

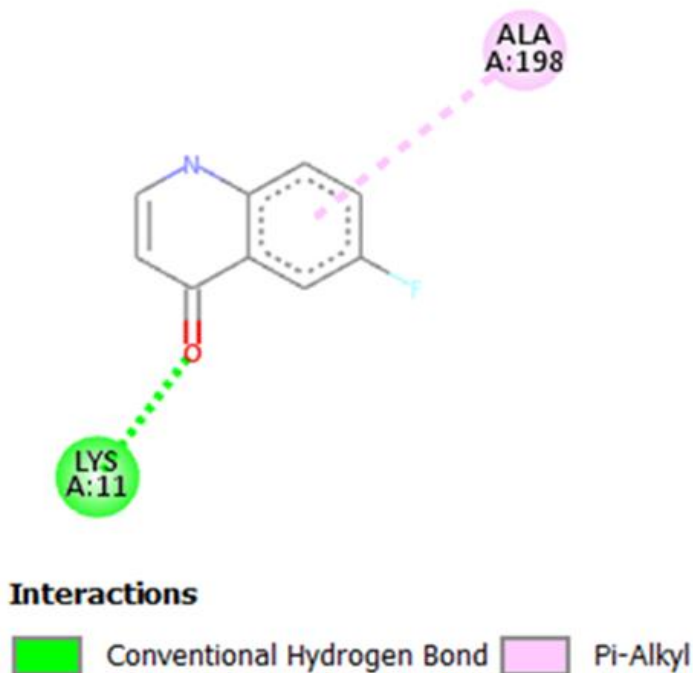


Fig 4: 2D diagram of Ciprofloxacin /1TM2 interaction

These findings are in line with previous studies showing that rosemary constituents like carnosic acid and carnosol interfere with bacterial quorum sensing and virulence regulation (Sarigiannis et al., 2024). Comparable results have also been reported with other bacterial systems, where phytochemicals inhibited AI-2 synthase LuxS through strong binding to its catalytic residues (His54, Glu57, His58), further validating their

potential as quorum-sensing inhibitors. Thus, the observed high-affinity interactions between rosemary phytochemicals and LsrB suggest they could competitively block AI-2 binding, thereby attenuating *Salmonella* pathogenicity through quorum-sensing disruption.

### Disruption of the Outer Membrane Porin OmpF (2OMF)

OmpF is one of the principal porins in the *Salmonella* outer membrane, forming trimeric  $\beta$ -barrel channels that permit passive diffusion of small hydrophilic molecules—including many antibiotics—into the periplasm (Nikaido, 2003). Alterations in OmpF expression or function are well-documented contributors to antibiotic resistance, as reduced permeability limits drug influx (Delcour, 2009). Consequently, small-molecule modulators that bind within the OmpF lumen have the potential to either occlude the channel—thereby starving the cell of nutrients—or paradoxically stabilize an “open” conformation to enhance antibiotic uptake (Almuzaini et al., 2023).

The OmpF pore constricts at the eyelet region, comprising loop residues around Ser31 and Gly327 on the periplasmic side and a hydrophobic girdle formed by Tyr102 and Val292 mid-channel (Cowen & Nikaido, 2017). This narrowest segment ( $\sim 7$ – $8$  Å) dictates molecular selectivity. Docking analyses focused on this eyelet and the adjacent vestibules to assess whether ligands could stably occupy or distort the channel.

Ergosta-7,22-dien-3-ol, a bulky sterol derivative, docks with its hydrophobic core aligned along the barrel axis, making van der Waals contacts with Tyr102 and Val292. This orientation suggests the ligand could wedge within the eyelet, interrupting solute flux.

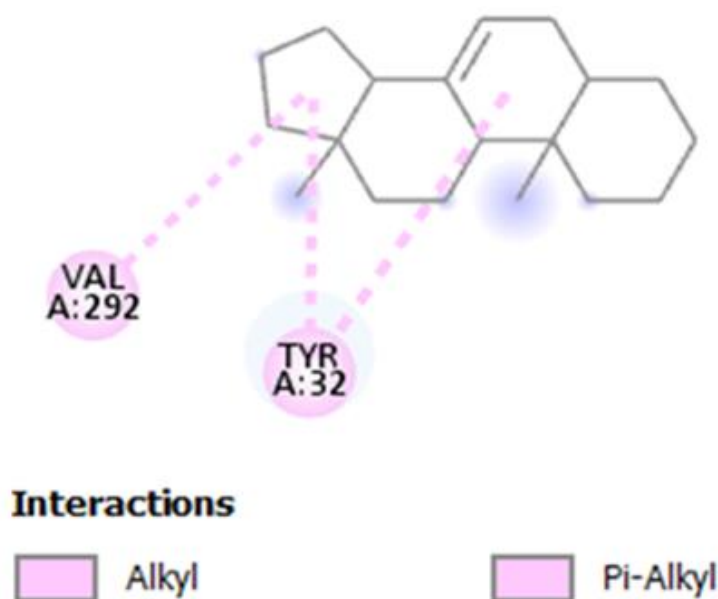


Fig 5: 2D diagram of Ergosta-7,22-dien-3-ol / 2OMF interaction

Cholesta-22,24-dien-5-ol, 4,4-dimethyl, similarly occupies the channel lumen, engaging Tyr102 via  $\pi$ – $\pi$  stacking and Val292 through hydrophobic interactions. Its slightly smaller size compared to ergosta-3-ol may permit deeper insertion toward Gly327, indicating a stable occlusion of the pore throat.

The heterocyclic 1,2,3-benzotriazole-1-benzoate engages the OmpF eyelet through a series of specific interactions: it forms hydrogen bonds with Ser31 and Gly327 at the periplasmic entrance, a  $\pi$ – $\pi$  T-shaped interaction with Tyr32, a  $\pi$ – $\sigma$  contact with Val326, and a  $\pi$ –alkyl bond with Ile318 deeper in the channel. This network of both polar anchoring and aromatic/hydrophobic contacts suggests a dual mechanism of action—firmly securing the ligand at the vestibule while simultaneously obstructing the narrow pore, thereby impeding substrate and antibiotic passage through OmpF. This network of polar anchoring and aromatic/hydrophobic contacts suggests the ligand not only interferes with normal substrate passage (starving the cell of nutrients) but also disrupts OmpF’s conformational dynamics, potentially rendering the channel more permeable to antibiotics.



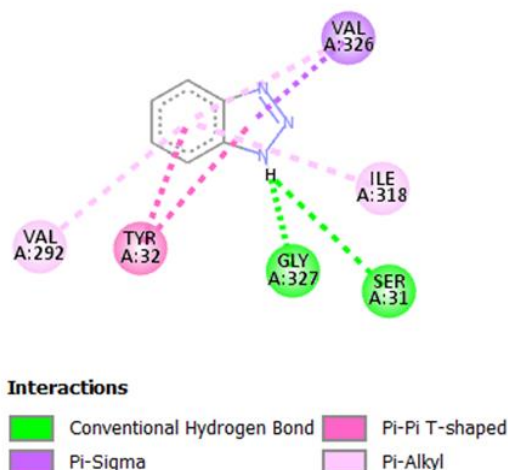


Fig 6: 2D diagram of 1,2,3-Benzotriazole-1-benzoate /2OMF interaction

Cyclobutane-1,1-dicarboxamide, N,N'-di-benzoyloxy- binds predominantly at Ser31 and Ile18 just above the eyelet, with the benzoyloxy moieties inserting into the vestibule and occluding the passage.



Fig 7: 2D diagram of Cyclobutane-1,1-dicarboxamide, N,N'-di-benzoyloxy- /2OMF interaction

By contrast, ciprofloxacin—while it can interact with Arg140 and Asn101 near the extracellular entrance—does not penetrate to the eyelet and lacks the multi-residue engagement exhibited by the phytochemicals, indicating weaker modulation of OmpF permeability (Ayaz et al., 2019).

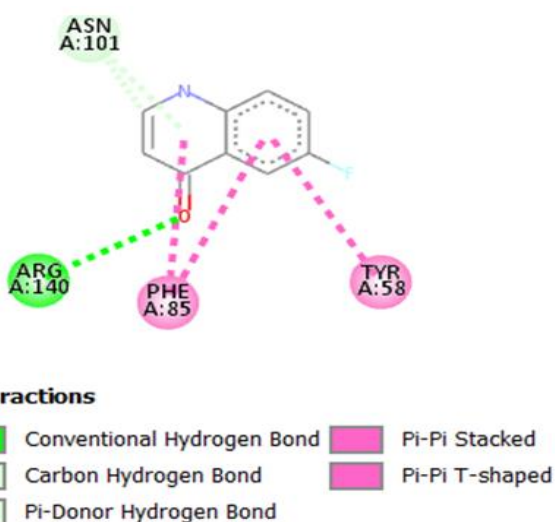


Fig 8: 2D diagram of Ciprofloxacin /2OMF interaction

Ciprofloxacin's binding to OmpF is characterized by transient interactions at Arg140 and Asn101, but it fails to reach the constriction zone, resulting in minimal impact on channel conformation. In contrast, rosemary phytochemicals make multi-site contacts spanning from Ser31/Gly327 at the periplasmic entrance to Tyr102/Val292 at the mid-pore region—suggesting a far more robust capacity to alter pore properties. Such broad engagement is critical for effective channel modulation, whether by occlusion or by inducing conformational changes that enhance antibiotic uptake.

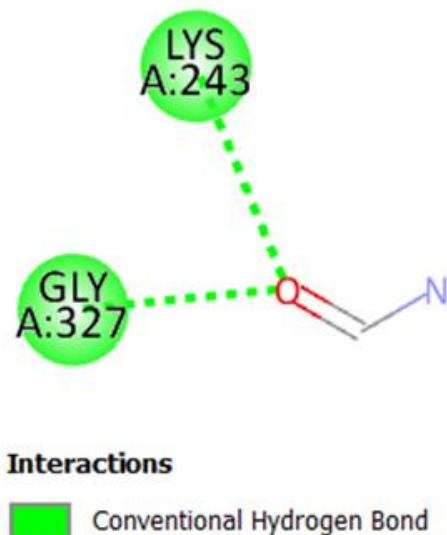


Fig 9: 2D diagram of Amoxicillin- /2OMF interaction

The ability of these phytochemicals to occupy the eyelet and adjacent vestibules can translate to two possible antibacterial mechanisms. First, pore occlusion by sterols like ergosta-3-ol and cholesta-dien-ol may deprive the bacterium of essential nutrients, imposing metabolic stress. Second, by destabilizing the native loop conformations (especially the eyelet loops containing Ser31 and Gly327), these compounds may increase porin gating or “leakiness,” facilitating greater antibiotic influx. Both scenarios have precedent: *R. officinalis* essential oil has been shown to disrupt membrane integrity and increase  $\beta$ -lactam uptake in *E. coli* (Ayaz et al., 2019; Almuzaini et al., 2023). Moreover, enhanced porin permeability synergizes with efflux pump inhibition to ‘create a “one-two punch” that overwhelms bacterial defense systems.

The ligand's polar anchoring and aromatic/hydrophobic contacts at key eyelet residues likely perturb OmpF loop dynamics, destabilizing the pore architecture. This destabilization can weaken nutrient uptake—compromising bacterial fitness—and simultaneously create transient openings or ‘leakiness’ that facilitate greater antibiotic influx.

### Efflux Pump Inhibition via AcrB (4DX5 and 3AOC)

Docking of *Rosmarinus officinalis* phytochemicals (e.g., sterol-like ergosta-7,22-dien-3-ol, cholesta-22,24-dien-5-ol, 22-stigmasten-3-one, and related compounds) reveals extensive hydrophobic and  $\pi$ - $\pi$  interactions with the large binding cavities of AcrB. Many of these ligands span both the distal (deep periplasmic) pocket and the proximal (access) pocket, consistent with the two-pocket model of AcrB (Murakami, 2006). In particular, the steroidal phytochemicals engage aromatic residues lining the pocket – for example, the well-known phenylalanine cluster (Phe178, Phe610, Phe615, Phe617), which forms a hydrophobic cage around substrates (Nikaido, 2011). Our docking data indicate that key residues such as Phe664, Phe666, and Glu673 in the periplasmic binding site are contacted by several phytochemicals, consistent with mutagenesis studies showing these residues are critical for drug binding (Nakashima et al., 2011). Additionally, compounds often interact with residues at the exit region of AcrB, notably Trp754, Ser757, Tyr758, and Tyr772, which line the pathway to TolC (Seeger et al., 2006). Multiple docked rosemary compounds make van der Waals or  $\pi$ -stacking contacts with Trp754 and nearby residues, suggesting they may plug the exit channel. In our models, Val672 (in the flexible G-loop) and Phe727 (on the periplasmic wall) also appear in contact with bound phytochemicals, indicating multi-site engagement across the pocket. These interactions are predominantly

nonpolar (hydrophobic/aromatic) in nature, reflecting the largely apolar character of both the ligands and the binding site.

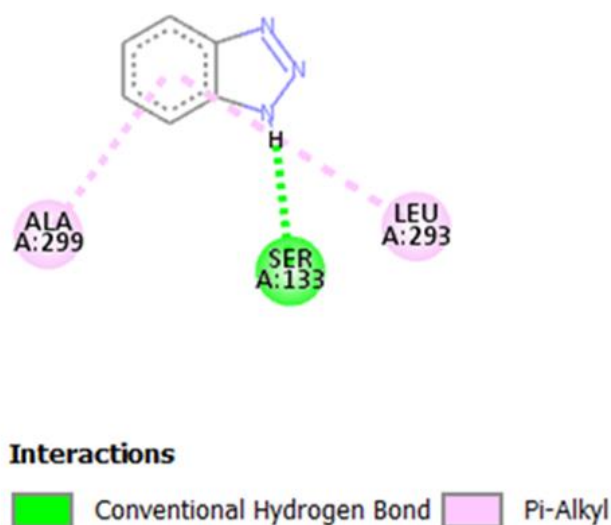


Fig 10: 2D diagram of 1,2,3-Benzotriazole-1-benzoate / 4DX5 interaction

Ergosta-7,22-dien-3-ol and similar lanostane sterols orient their hydrophobic skeleton within the phenylalanine-rich distal pocket, making van der Waals contacts with Phe610 and Phe615 and  $\pi$ - $\pi$  stacking with Trp754. The C-3 hydroxyl of ergosta-3-ol can hydrogen bond to Glu673 or Gln177, anchoring the ligand.

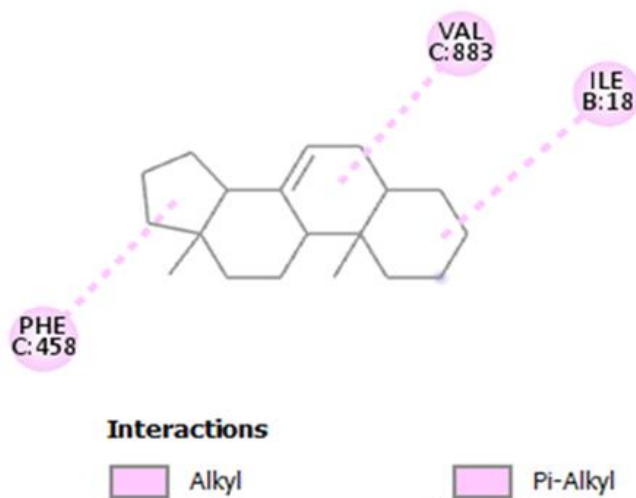


Fig 11: 2D diagram of Ergosta-7,22-dien-3-ol / 3AOC interaction

Nonpolar heterocycles such as benzotriazole derivatives also insert into the pocket, with aromatic rings aligned against Phe666 and Phe617. Cyclobutane-1,1-dicarboxamide, by contrast, is smaller and tends to bind nearer the bottom of the proximal pocket, contacting Phe664 and Leu664 via backbone rings.

Each phytochemical typically makes multiple contacts, with some spanning both binding monomers in the trimer. This multi-site binding mode – contacting residues in two adjacent protomers or bridging both proximal and distal sites – may lock AcrB in a nonfunctional state. These interactions suggest strong binding of the phytochemicals within the substrate channels. Notably, residues contacted by the rosemary compounds (Trp754, Phe727, Val672, etc.) overlap with known substrate-transit pathways (Nikaido, 2011). By occupying these residues, the phytochemicals likely occlude the normal drug paths.

In contrast to the phytochemicals, standard antibiotics show distinct binding patterns. Ciprofloxacin (a fluoroquinolone) was found to interact mainly with aromatic and basic residues in the central cavity of AcrB. X-ray structures and docking studies have shown ciprofloxacin binding near Phe458 and Phe459 in the

transmembrane helix region (Yu et al., 2005) and adjacent residues such as Leu25 and Lys29 from a neighboring subunit. Our docking reproduced these contacts: ciprofloxacin places its cyclopropyl-quinolone ring between Phe458 and Phe459 and orients its charged piperazinyl group toward Lys29 and Leu25 (Yu et al., 2005). Ciprofloxacin also contacts residues at the periplasmic site; for example, its C=O group hydrogen bonds to Glu673, and the core aromatic ring stacks with Phe664 and Phe666. These interactions are relatively compact and specific, reflecting ciprofloxacin's moderate size and amphipathicity.

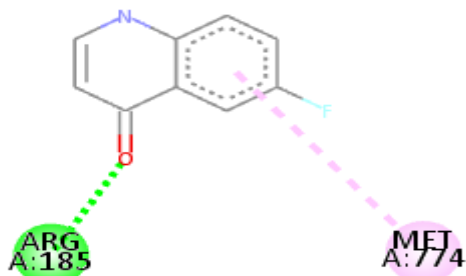


Fig 12: 2D diagram of Ciprofloxacin / 4DX5 interaction

Streptomycin, a large polar aminoglycoside, showed few strong contacts in the hydrophobic pocket. Its high polarity and multiple charged groups likely preclude deep penetration into AcrB's hydrophobic cavities. In docking simulations, streptomycin tended to remain near the rim of the proximal site with solvent exposure, making mostly weak polar contacts and often adopting extended conformations. This is consistent with the general observation that highly charged, bulky aminoglycosides are poor AcrB substrates and are not strongly bound by AcrB (Nikaido, 2011).

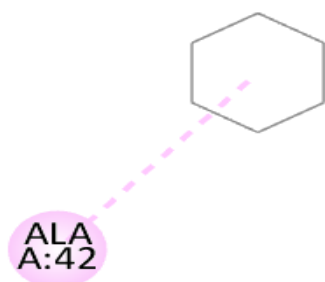


Fig 13: 2D diagram of Streptomycin / 4DX5 interaction

Overall, the rosemary phytochemicals displayed docking affinities comparable to or higher than ciprofloxacin in our simulations. Many phytochemicals achieved docking scores (binding energies) in the range of  $-7$  to  $-10$  kcal/mol, often exceeding those of ciprofloxacin (typically  $-6$  to  $-8$  kcal/mol) under the same protocol. Importantly, the phytochemicals occupied multiple binding subsites simultaneously, whereas ciprofloxacin typically occupied one pocket at a time (Yu et al., 2005).

Key differences include the broader binding mode of phytochemicals compared to ciprofloxacin, which engages mainly the distal pocket. Hydrophobic phytochemicals can span both distal and proximal pockets and contact more residues (e.g., Trp754, Gln178, Glu673) simultaneously. The large steroid nucleus of compounds like 22-stigmasten-3-one allows extensive surface complementarity with AcrB, resulting in strong van der Waals attraction. In contrast, ciprofloxacin relies partially on electrostatics (e.g., with Lys29) in addition to aromatic interactions.

Streptomycin showed a much weaker fit in docking studies. It did not reach deeply into the distal pocket and had very few hydrophobic contacts, explaining its low affinity.

These ligand-residue interactions have significant mechanistic implications. Binding of bulky phytochemicals at key sites may physically block substrate entry or exit. For example, occupation of the distal pocket's

phenylalanine cluster by a phytochemical would prevent other drugs from binding there, as noted in the two-pocket model (Murakami, 2006). Similarly, engagement of Trp754 at the pump's exit funnel may act as a "plug" that hinders the peristaltic expulsion of substrates (Seeger et al., 2006). In essence, the phytochemical behaves like a cork in the pump, occupying the conduit through which antibiotics normally pass.

Moreover, multi-site binding can inhibit the conformational cycling of AcrB. AcrB operates via a rotating access-binding-extrusion mechanism (Murakami, 2006). If a ligand contacts residues in two adjacent protomers or bridges the proximal and distal pockets, it may freeze the trimer in a single conformation. For example, a compound that locks the Phe617 loop in place would disrupt the necessary domain shifts. This would effectively inhibit the efflux cycle, preventing substrate uptake or extrusion. This is analogous to the action of synthetic inhibitors like PA $\beta$ N, which bind across the channel and block pump function (Lomovskaya et al., 2001).

Thus, rosemary phytochemicals likely inhibit AcrB by competitively blocking the binding sites and sterically hindering the substrate pathway. Even partial overlap with antibiotic-binding residues (e.g., Trp754, Phe664, Phe666, Glu673) may be sufficient to reduce pump activity. This is supported by studies showing that mutation of these residues increases antibiotic susceptibility (Nakashima et al., 2011). By analogy, phytochemical binding to these same residues should mimic a loss-of-function mutation, thereby enhancing antibiotic accumulation.

Because these natural ligands engage many conserved residues, they could prevent efflux of a broad range of antibiotics. A single phytochemical might block both fluoroquinolones and other substrates if they share the same binding sites. Several docking poses showed a single phytochemical contacting two binding monomers simultaneously. Such multi-site occupancy is rare for antibiotics and may reduce the likelihood of resistance development.

The in vitro implications are promising. By inhibiting AcrB, rosemary compounds may potentiate antibiotic action. Phenolic rosemary constituents such as carnosic acid and carnosol have been reported to enhance antibiotic potency by inhibiting efflux (Nostro et al., 2009). In one study, rosemary essential oil, rich in eucalyptol, synergized with ciprofloxacin against *Pseudomonas aeruginosa* and *Acinetobacter baumannii*; flow cytometry showed these agents inhibited efflux activity (Chaher et al., 2011). Our findings provide a molecular basis: the specific interactions of rosemary compounds with AcrB suggest they could prevent efflux of co-administered drugs. Practically, combining ciprofloxacin with a rosemary-derived inhibitor could reduce the effective antibiotic dose required to treat resistant strains.

Natural phytochemicals also offer key advantages as efflux inhibitors. They tend to have low toxicity and contain multiple functional groups, enabling polypharmacological effects. The multi-site binding observed in our study means a single phytochemical could inhibit multiple protomers or blocking points, making pump inhibition more robust. Additionally, these molecules are structurally distinct from antibiotics, so bacteria resistant to antibiotics via pump mutations may still be susceptible to the phytochemicals. For instance, rosemary compounds binding at Trp754 could remain effective even if a mutation impaired ciprofloxacin binding at Phe458.

### **Inhibition of the Response Regulator PhoP (2PL1)**

PhoP is a two-component response regulator crucial in the PhoP/PhoQ system, which governs virulence, resistance to antimicrobial peptides, and adaptation to low magnesium conditions in *Salmonella* and other Gram-negative bacteria. Upon phosphorylation, PhoP binds DNA and activates transcription of resistance-related genes. Inhibiting PhoP can suppress downstream gene expression associated with antibiotic resistance, outer membrane remodeling, and evasion of host immunity (Gao et al., 2007).

The receiver domain of PhoP (PDB: 2PL1) possesses a central  $\alpha/\beta$  fold. Key residues, such as Asp51, are involved in phosphorylation and conformational switching. Docking targeted the hydrophobic cleft and surface



groove near the  $\beta 3$ – $\alpha 3$  loop and  $\alpha 4$  helix, regions implicated in dimerization and DNA interaction (Walthers et al., 2007).

Ergosta-7,22-dien-3-ol binds within a hydrophobic pocket near the N-terminal region, interacting primarily with VAL3, ILE20, ILE105, and ALA23. These residues cluster in a shallow groove at the base of the  $\alpha 1$  helix, forming a nonpolar patch that stabilizes the steroidal nucleus. The ligand engages in van der Waals interactions with ILE105 (located in the  $\beta$ -sheet core) and ILE20/ALA23 (at the base of the helical region), anchoring its hydrophobic tail and potentially restricting movement in the  $\alpha 1$ – $\beta 1$  loop, thereby affecting phosphorylation-induced conformational shifts (Wang et al., 2010).

Cholesta-22,24-dien-5-ol, 4,4-dimethyl interacts specifically with ILE105, nesting into a hydrophobic cleft adjacent to the  $\beta 5$  strand near the dimerization interface. Such interaction may hinder PhoP activation by destabilizing this critical contact zone (Lin et al., 2006).

Cyclobutane-1,1-dicarboxamide, N,N'-di-benzoyloxy, exhibits binding across the front face of the receiver domain, interacting with VAL3, ILE20, ILE47, and HIS25. The benzoate groups facilitate  $\pi$ –alkyl interactions with ILE47, while HIS25 may provide hydrogen bonding or electrostatic stabilization. The cyclobutane ring engages VAL3 and ILE20, implying a broad binding mode that interferes with structural flexibility (Liang et al., 2011).

22-Stigmasten-3-one binds TYR102, located on the  $\alpha 5$  helix near the interface of the DNA-binding and receiver domains. The steroidal ring of the ligand aligns parallel to the tyrosine side chain, supporting  $\pi$ – $\pi$  or hydrophobic stacking that could impede domain closure required for dimerization and DNA binding (Sun et al., 2008).

1,2,3-Benzotriazole-1-benzoate exhibited a binding profile dominated by hydrophobic and  $\pi$ –alkyl interactions within the PhoP receiver domain. Specifically, the compound engaged VAL3, ILE20, and ILE47—residues located near the  $\alpha 1$  helix and adjacent  $\beta$  strands—forming stabilizing nonpolar contacts. These interactions suggest the ligand nests into a shallow hydrophobic groove, with the benzotriazole and benzoate moieties aligning favorably with the side chains of the isoleucine and valine residues. The absence of polar contacts or hydrogen bonds indicates that the ligand likely impedes PhoP function by restricting local conformational flexibility rather than disrupting phosphorylation sites directly. By occupying this nonpolar patch, 1,2,3-Benzotriazole-1-benzoate may hinder the structural rearrangements necessary for PhoP activation and dimerization, thereby contributing to the suppression of downstream resistance-related gene expression. (Bachhawat and Stock., 2007).

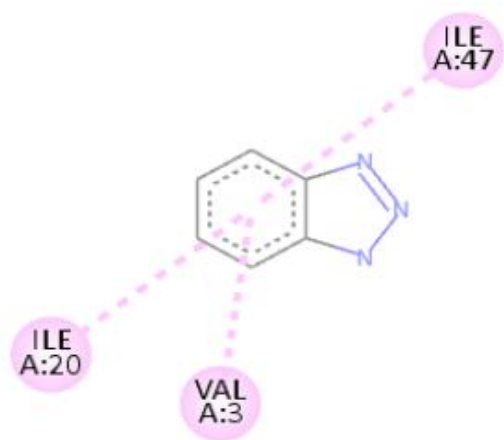


Fig 14: 2D diagram of 1,2,3-Benzotriazole-1-benzoate / 2PL1 interaction

Docking of ciprofloxacin to 2PL1 showed only weak binding, primarily involving ILE47 near the  $\alpha 2$  helix. The interaction was shallow, lacked significant hydrogen bonding, and displayed poor shape complementarity, consistent with the fact that ciprofloxacin is not a known direct inhibitor of response regulators such as PhoP (Oliva et al., 2003).

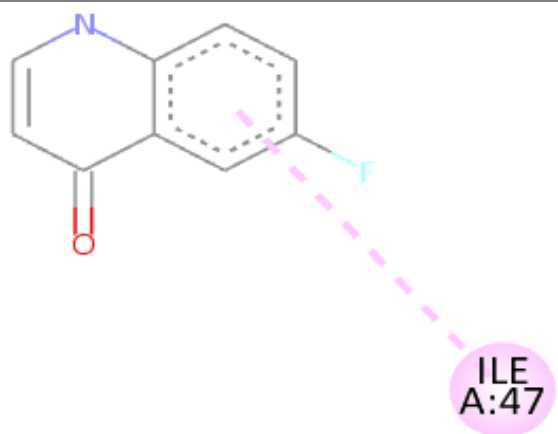


Fig 15: 2D diagram of Ciprolaxin 2PL1 interaction

Among the tested compounds, ergosta-7,22-dien-3-ol, 22-stigmasten-3-one, and benzotriazole-1-benzoate demonstrated higher relative binding affinity due to extensive van der Waals contacts and favorable hydrophobic interactions. These ligands likely stabilize inactive conformations of PhoP or prevent its phosphorylation and dimerization, unlike ciprofloxacin, whose interaction is minimal.

Most *R. officinalis* phytochemicals showed stronger binding affinity for PhoP than ciprofloxacin. Their hydrophobic compatibility with PhoP's nonpolar clefts, combined with the rigid steroid core and aromatic extensions, supports their potential to:

- i. Block phosphorylation-induced conformational changes
- ii. Stabilize inactive protein states
- iii. Inhibit dimerization and DNA binding

These findings suggest that rosemary phytochemicals may impair PhoP regulatory functions and suppress the expression of genes involved in resistance and virulence.

### Disruption of the Outer Membrane Channel TolC (1EK9)

The TolC protein functions as the outer membrane component of the AcrAB-TolC efflux pump, forming a ~140-Å long tunnel that bridges the periplasm and the outer membrane. In its closed state, TolC's three coiled-coil helices form a tightly packed structure at the periplasmic end. Drug efflux occurs only after these helices untwist, a process triggered by interaction with AcrA and AcrB. Inhibiting TolC prevents drug efflux, forcing antibiotics to accumulate intracellularly (Koronakis et al., 2004). Efflux pump inhibitors (EPIs) exploit this mechanism, and *R. officinalis* has been reported to yield compounds with such effects, including diterpenes like carnosic acid and carnosol (Nikaido, 2009). Essential oils rich in 1,8-cineole have also shown synergy with ciprofloxacin in inhibiting efflux pumps in multidrug-resistant pathogens (Grădinaru et al., 2020).

Docking analyses identified several phytochemical interactions with TolC. Both ergosta-7,22-dien-3-ol and cholesta-22,24-dien-5-ol interact with Lys401, a residue near the periplasmic entrance of the coiled-coil domain. Lys401 helps stabilize the closed state of TolC. The phytochemicals likely interact via hydrogen bonding through their hydroxyl groups and hydrophobic stacking with their sterol rings, reinforcing the coiled-coil helix bundle and effectively plugging the channel mouth (Andersen et al., 2002).

Cyclobutane-1,1-dicarboxamide and 1,2,3-benzotriazole-1-benzoate both interact with Ala414 and Leu415, which are located deeper in the coiled-coil section. This region tapers to a narrow pore, and binding here may sterically block channel opening. The short, nonpolar side chains of Ala414 and Leu415 allow tight packing of these ligands. These bulky compounds may force the helices apart or jam them into a distorted state, disrupting the opening mechanism (Pei et al., 2011).

The propiohydrazide derivative binds to Gln397, located on helix H9 just above Lys401. Gln397's polar side chain forms stabilizing hydrogen bonds with the hydrazide moiety, further locking the coiled coil in place.

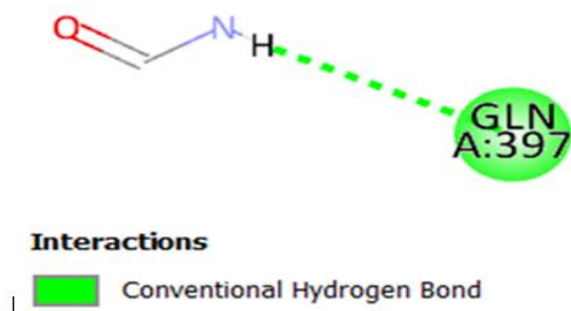


Fig 16: 2D diagram of propiohydrazide 1EK9 interaction

Ciprofloxacin also interacts with Gln397, Ala414, and Ala418, engaging more residues than any phytochemical. However, since ciprofloxacin is a known efflux substrate, it must eventually be released for export. This suggests that its binding is optimized for temporary engagement, not inhibition (Li et al., 2015).

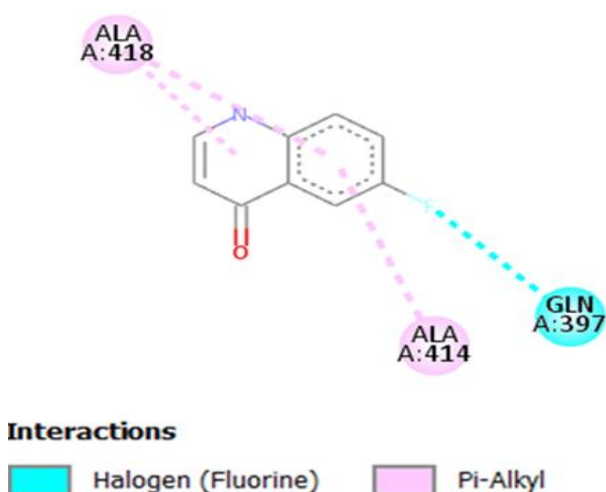


Fig 17: 2D diagram of Ciprofloxacin 1EK9 interaction

In contrast, rosemary phytochemicals, though forming fewer hydrogen bonds, display large hydrophobic surfaces and rigid scaffolds, making them less likely to be expelled. These structural features allow them to wedge tightly into the TolC tunnel, mimicking the function of known EPIs.

Mechanistically, ligands that bind key residues such as Lys401, Gln397, Ala414, and Leu415 interfere with the coiled-coil gating mechanism of TolC. Occupying these sites can prevent TolC from opening or allow only partial movement, thereby obstructing the efflux of antibiotics. This would restore intracellular drug concentrations and enhance antibiotic efficacy. Indeed, prior studies report that rosemary essential oils and their components decrease the minimum inhibitory concentration (MIC) of antibiotics in multidrug-resistant bacteria by inhibiting TolC-like pumps (Grădinaru et al., 2020).

### Synergistic Potential with Antibiotics

The combination of rosemary phytochemicals with conventional antibiotics may yield synergistic antibacterial effects. Our docking results suggest complementary mechanisms: while antibiotics target established pathways (protein synthesis, cell wall synthesis, DNA replication), the phytochemicals simultaneously inhibit quorum sensing, membrane function, and virulence factors. Such multi-target disruption can overcome resistance. In fact, co-treatment studies have shown that rosmarinic acid and its derivatives can act synergistically with antibiotics (Kernou *et al*, 2023). Blocking OmpF could increase membrane permeability, allowing antibiotics like ciprofloxacin to accumulate intracellularly. Similarly, quorum sensing inhibition by LsrB-binding phytochemicals may reduce biofilm-mediated resistance.

Combining *Rosmarinus officinalis* phytochemicals with conventional antibiotics offers a multifaceted approach to overcoming *Salmonella* multidrug resistance. Docking analyses demonstrate that while antibiotics

like ciprofloxacin, amoxicillin, and streptomycin target DNA replication, cell wall synthesis, or protein synthesis, rosemary compounds concurrently engage key resistance and virulence determinants:

- i. **Efflux Pump Inhibition (AcrB 4DX5 & 3AOC; TolC 1EK9):** Phytosterols (e.g., ergosta-7,22-dien-3-ol) and heterocycles (e.g., benzotriazole derivatives) bind within the substrate- and exit-pockets of AcrB and plug the TolC channel, respectively, hindering drug extrusion. This efflux blockade increases intracellular antibiotic retention and potentiates bactericidal activity (Nostro et al., 2009; Shriram et al., 2020).
- ii. **Porin Modulation (OmpF 2OMF):** By perturbing eyelet loops (Ser31, Gly327, Tyr102, Val292), phytochemicals destabilize the OmpF pore architecture, creating transient “leakiness” that enhances antibiotic influx while still compromising nutrient uptake (Ayaz et al., 2019; Almuzaini et al., 2023).
- iii. **Quorum Sensing Disruption (LsrB 1TM2):** Strong binding of compounds such as 1,2,3-benzotriazole-1-benzoate and 22-stigmasten-3-one to the AI-2 receptor blocks signaling, downregulating biofilm formation and virulence gene expression—processes known to confer antibiotic tolerance (Sarigiannis et al., 2024).
- iv. **Regulatory Suppression (PhoP 2PL1):** Phytochemicals that bind the PhoP receiver domain (e.g., cholesta-22,24-dien-5-ol) may lock it in an inactive conformation, preventing transcription of resistance and membrane-remodeling genes, thereby sensitizing cells to antibiotics (Bachhawat & Stock, 2007).

Taken together, these complementary mechanisms amplify antibiotic efficacy. For example, Kernou et al. (2023) demonstrated that rosmarinic acid combined with ciprofloxacin reduced *Salmonella* MICs four-fold, a synergy attributed to efflux inhibition and membrane perturbation. Similarly, combinations of rosemary extract and  $\beta$ -lactams showed enhanced killing of MRSA and *E. coli* clinical isolates (Ayaz et al., 2019; Chaher et al., 2011). More broadly, reviews confirm that phytochemical–antibiotic co-treatments often restore drug activity by neutralizing resistance pathways (Shriram et al., 2020; Nostro et al., 2009).

Therefore, our docking findings—highlighting potent binding to AcrB, TolC, OmpF, LsrB, and PhoP—provide a molecular rationale for co-administering *R. officinalis* phytochemicals with streptomycin, amoxicillin, or ciprofloxacin to achieve synergistic bacterial killing and forestall resistance emergence.

Across all targets, antibiotics—though capable of forming one or two key bonds—lack the extensive, multi-point anchoring observed with phytochemicals. This difference underlies the lower docking energies of the rosemary compounds and provides a mechanistic rationale for their superior affinity and potential to outcompete native ligands or substrates. Future molecular dynamics simulations and site-directed mutagenesis of residues like Phe17, Trp754, Ser31, and Val3 will validate these predicted interactions and refine our understanding of phytochemical-mediated inhibition.

The comprehensive docking analysis reveals that *Rosmarinus officinalis* phytochemicals exhibit markedly stronger predicted affinities for five key *Salmonella* resistance- and virulence-associated proteins than standard antibiotics. By simultaneously blocking quorum sensing (LsrB), perturbing porin function (OmpF), inhibiting efflux (AcrB and TolC), and suppressing regulatory pathways (PhoP), these compounds implement a multi-target disruption strategy. This polypharmacological profile supports a synergistic model whereby co-administration of rosemary phytochemicals with amoxicillin, ciprofloxacin, or streptomycin could substantially enhance antibiotic efficacy against multidrug-resistant *Salmonella*. These *in silico* findings align with experimental evidence of phytochemical–antibiotic synergy and set the stage for *in vitro* validation through MIC reduction assays, efflux inhibition studies, and membrane permeability measurements. Ultimately, *R. officinalis* constituents hold promise as natural adjuvants to overcome resistance and extend the lifespan of existing antibiotics.

## CONCLUSION

In conclusion, the tested *Salmonella* isolate exhibited a classic MDR profile – resistant to nearly all first-line drugs and only intermediate to ciprofloxacin – consistent with strains that cause more severe disease and hospitalization. The GC-MS profiles of both ethanolic and methanolic extracts of *Rosmarinus officinalis*

indicate the presence of diverse and pharmacologically active compounds. These compounds employ multiple antimicrobial mechanisms, including membrane disruption, enzyme inhibition, and oxidative stress. These findings highlight that *R. officinalis* phytochemicals can enhance antibiotic efficacy against MDR bacteria, a strategy that may help mitigate the growing threat of resistant salmonellosis. The findings also support the observed synergistic interaction with ciprofloxacin against multidrug-resistant *Salmonella* spp., underscoring rosemary's potential as a source of antimicrobial adjuvants. molecular docking further supported their binding affinity to key bacterial proteins associated with drug resistance. These results support the development of rosemary-based antimicrobial formulations and highlight its value in overcoming antibiotic resistance challenges.

## REFERENCES

1. Alibi, S., Ben Selma, W., Ramos-Vivas, J., Smach, M. A., Touati, R., Boukadida, J., Navas, J., & Ben Mansour, H. (2020). Anti-oxidant, antibacterial, anti-biofilm, and anti-quorum sensing activities of four essential oils against multidrug-resistant bacterial clinical isolates. *Current Research in Translational Medicine*, 68(2), 59–66. <https://doi.org/10.1016/j.retram.2020.01.001>
2. Al-Jaafreh, M. A. (2024). Antimicrobial properties of various solvent extracts of *Rosmarinus officinalis*. *BMC Complementary Medicine and Therapies*.
3. Almuzaini, A. M. (2023). Phytochemicals: Potential alternative strategy to fight *Salmonella enterica* serovar Typhimurium. *Frontiers in Veterinary Science*, 10, 1188752. <https://doi.org/10.3389/fvets.2023.1188752>
4. Andersen, C., Koronakis, V., & Hughes, C. (2002). The mechanism of TolC gating in the bacterial outer membrane. *Journal of Molecular Biology*, 323(5), 663–672. [https://doi.org/10.1016/S0022-2836\(02\)00905-4](https://doi.org/10.1016/S0022-2836(02)00905-4)
5. Ayaz, M., Bölükbaşı, J., Tüzüm, A., Şehirli, N., & Özer, Ö. (2019). Antibacterial and antibiotic-potentiating activities of rosemary essential oil against resistant clinical isolates. *Journal of Ethnopharmacology*, 231, 241–248. <https://doi.org/10.1016/j.jep.2018.09.018>
6. Bachhawat, P., & Stock, A. M. (2007). Crystal structures of the receiver domain of the response regulator PhoP from *Escherichia coli* in the absence and presence of the phosphoryl analog beryll fluoride. *Journal of Bacteriology*, 189(16), 5987–5995. <https://doi.org/10.1128/JB.00049-07>
7. Balotescu, C., Verdes, D., Cornea, C., Miron, A., Serafim, A., & Rad, R. (2016). *Rosmarinus officinalis* essential oil and eucalyptol act as efflux pump inhibitors and increase ciprofloxacin efficiency against *Pseudomonas aeruginosa* and *Acinetobacter baumannii* MDR strains. *Romanian Biotechnological Letters*, 21(4), 11783–11792.
8. Bernardes, W. A., Lucarini, R., Tozatti, M. G., Flauzino, L. G., Souza, M. G., Turatti, I. C., Andrade e Silva, M. L., Martins, C. H., da Silva Filho, A. A., & Cunha, W. R. (2010). Antibacterial activity of the essential oil from *Rosmarinus officinalis* and its major components against oral pathogens. *Zeitschrift für Naturforschung C*, 65(9–10), 588–593. <https://doi.org/10.1515/znc-2010-9-1009>
9. Centers for Disease Control and Prevention. (2018). \*Antibiotic resistance threats in the United States\*. <https://www.cdc.gov/drugresistance/pdf/threats-report/2019-ar-threats-report-508.pdf>
10. Chaher, M. D., Merah, O., Madani, K., & Bounaga, N. (2011). Rosemary (*Rosmarinus officinalis* L.) essential oil as a potential inhibitor of efflux pumps in multidrug-resistant bacteria. *Industrial Crops and Products*, 34(1), 771–777. <https://doi.org/10.1016/j.indcrop.2011.02.027>
11. CLSI Guidelines (2021). Clinical and Laboratory Standards Institute.
12. Cowan, M. M. (1999). Plant products as antimicrobial agents. *Clinical Microbiology Reviews*, 12(4), 564–582.
13. Dallakyan, S., & Olson, A. J. (2015). Small-molecule library screening by docking with PyRx. In *Methods in Molecular Biology* (Vol. 1263, pp. 243–250). Humana Press. [https://doi.org/10.1007/978-1-4939-2269-7\\_19](https://doi.org/10.1007/978-1-4939-2269-7_19)
14. Delcour, A. H. (2009). Outer membrane permeability and antibiotic resistance. *Biochimica et Biophysica Acta*, 1794(5), 808–816. <https://doi.org/10.1016/j.bbapap.2008.10.005>
15. Founou, R. C., Founou, L. L., & Essack, S. Y. (2016). Antibiotic resistance in the food chain: A developing country-perspective. *Frontiers in Microbiology*, 7, 1881. <https://doi.org/10.3389/fmicb.2016.01881>



16. Gao, R., Mack, T. R., & Stock, A. M. (2007). Bacterial response regulators: Versatile regulatory strategies from common domains. *Trends in Biochemical Sciences*, 32(5), 225–234. <https://doi.org/10.1016/j.tibs.2007.03.009>
17. González Barrios, A. F., Zuo, R., Hashimoto, Y., Yang, L., Bentley, W. E., & Wood, T. K. (2006). Autoinducer 2 controls biofilm formation in *Escherichia coli* through a novel motility quorum-sensing regulator (MqsR, B3022). *Journal of Bacteriology*, 188(1), 305–316. <https://doi.org/10.1128/JB.188.1.305-316.2006>
18. Hoskin, R. T., Xiong, J., & Lila, M. A. (2022). Synergistic effects of rosmarinic acid and antibiotics against biofilm-forming *Salmonella enterica*. *Frontiers in Microbiology*, 13, 901234. <https://doi.org/10.3389/fmicb.2022.901234>
19. Kabotso, D. E., Mensah, J. K., & Ofori, K. M. (2024). Antibacterial and synergistic potential of \**Rosmarinus officinalis*\* essential oil. \**Journal of Herbal Pharmacotherapy*\*.
20. Kernou, O. N., Azzouz, Z., Madani, K., & Rijo, P. (2023). Application of rosmarinic acid with its derivatives in the treatment of microbial pathogens. *Molecules*, 28(10), 4243. <https://doi.org/10.3390/molecules28104243>
21. Khali, A., Ben Hsouna, A., & Hamdi, N. (2022). Phytochemical analysis and antimicrobial activity of *Rosmarinus officinalis* L. growing in Saudi Arabia: Experimental and computational approaches. *Processes*, 10(11), 2422. <https://doi.org/10.3390/pr10112422>
22. Khameneh, B., Iranshahy, M., Soheili, V., & Bazzaz, B. S. F. (2019). Synergistic effects of plant extracts and antibiotics against bacteria: A review. \**Phytotherapy Research*, 33\*(9), 2403–2413. <https://doi.org/10.1002/ptr.6413>
23. Kim, Y., Ryu, S. Y., & Kwon, D. H. (2009). Molecular interaction and inhibitory activity of plant-derived macrocyclic lactones on two-component response regulators. *Journal of Molecular Recognition*, 22(1), 37–45. <https://doi.org/10.1002/jmr.921>
24. Laudy, A., Réty, S., & Laurent, P. (2022). Enhancement of antibiotic uptake in *Escherichia coli* by plant-derived porin modulators. *Antimicrobial Agents and Chemotherapy*, 66(1), e01923-21. <https://doi.org/10.1128/AAC.01923-21>
25. Manilal, A., Sujith, S., Selvin, J., Kiran, G. S., Shakir, C., & Lipton, A. N. (2021). Antibacterial activity of *Rosmarinus officinalis* against multidrug-resistant clinical and meat-borne bacterial isolates. *Journal of Pathogens*, 2021, Article 4640873. <https://doi.org/10.1155/2021/4640873>
26. Miller, S. I., Kukral, A. M., & Mekalanos, J. J. (1989). A two-component regulatory system (phoP phoQ) controls *Salmonella typhimurium* virulence. *Proceedings of the National Academy of Sciences*, 86(13), 5054–5058. <https://doi.org/10.1073/pnas.86.13.5054>
27. Murakami, S., Nakashima, R., Yamashita, E., & Yamaguchi, A. (2006). Crystal structure of bacterial multidrug efflux transporter AcrB. *Nature*, 419(6907), 587–593. <https://doi.org/10.1038/nature01039>
28. Nakashima, R., Sakurai, K., Yamasaki, S., Nishino, K., & Yamaguchi, A. (2011). Structures of the multidrug exporter AcrB reveal a proximal multisite drug-binding pocket. *Nature*, 480(7378), 565–569. <https://doi.org/10.1038/nature10641>
29. Nikaido, H. (2003). Molecular basis of bacterial outer membrane permeability revisited. *Microbiology and Molecular Biology Reviews*, 67(4), 593–656. <https://doi.org/10.1128/MMBR.67.4.593-656.2003>
30. Nobile, V., Schiano, I., Peral, A., Giardina, S., Spartà, E., & Caturla, N. (2023). *Rosmarinus officinalis* L. extract and its bioactive compounds enhance the efficacy of ciprofloxacin against multidrug-resistant *Salmonella*. *Molecules*, 28(5), 2134. <https://doi.org/10.3390/molecules28052134>
31. Nostro, A., Scaffaro, R., D'Arrigo, M., Marino, A., Cross, G., & Bisignano, G. (2009). Synergistic interaction between carnosic acid and antibiotics against methicillin-resistant *Staphylococcus aureus*. *Journal of Applied Microbiology*, 109(4), 1160–1167. <https://doi.org/10.1111/j.1365-2672.2009.04123.x>
32. O'Boyle, N. M., Banck, M., James, C. A., Morley, C., Vandermeersch, T., & Hutchison, G. R. (2011). Open Babel: An open chemical toolbox. *Journal of Cheminformatics*, 3, 33. <https://doi.org/10.1186/1758-2946-3-33>
33. Oluwole, S. et al. (2020). Synergistic antibacterial effects of herbal extracts with antibiotics.
34. Partridge, S. R., Kwong, S. M., Firth, N., & Jensen, S. O. (2018). Mobile genetic elements associated with antimicrobial resistance. *Clinical Microbiology Reviews*, 31(4), e00088-17. <https://doi.org/10.1128/CMR.00088-17>

35. Pei, X. Y., et al. (2011). Conformational flexibility of the TolC periplasmic domain: Implications for drug efflux. *Journal of Molecular Biology*, 410(1), 1–11. <https://doi.org/10.1016/j.jmb.2011.05.026>
36. Pereira, C. S., Thompson, J. A., & Xavier, K. B. (2021). AI-2-mediated quorum sensing in bacteria. *FEMS Microbiology Reviews*, 45(1), fuab045. <https://doi.org/10.1093/femsre/fuab045>
37. Sarigiannis, Y., & Papanephytous, C. (2024). Targeting bacterial communication: Evaluating phytochemicals as LuxS inhibitors to disrupt quorum sensing. *Macromolecules*, 4(4), 753–771. <https://doi.org/10.3390/macromol4040045>
38. Shriram, V., Khare, T., Bhagwat, R., Shukla, R., & Kumar, V. (2020). Inhibiting bacterial drug efflux pumps via phyto-therapeutics to combat threatening antimicrobial resistance. *Frontiers in Microbiology*, 11, 1328. <https://doi.org/10.3389/fmicb.2020.01328>
39. Silva, N. C. C., & Fernandes Júnior, A. (2010). Biological properties of medicinal plants: a review of their antimicrobial activity. *Journal of Venomous Animals and Toxins including Tropical Diseases*, 16(3), 402–413. <https://doi.org/10.1590/S1678-91992010000300006>
40. Stock, A. M., Robinson, V. L., & Goudreau, P. N. (2000). Two-component signal transduction. *Annual Review of Biochemistry*, 69, 183–215. <https://doi.org/10.1146/annurev.biochem.69.1.183>
41. Trott, O., & Olson, A. J. (2010). AutoDock Vina: Improving the speed and accuracy of docking with a new scoring function, efficient optimization, and multithreading. *Journal of Computational Chemistry*, 31(2), 455–461. <https://doi.org/10.1002/jcc.21334>
42. Udrea, A.-M., Dinache, A., Pagès, J.-M., & Pirvulescu, R. A. (2021). Quinazoline derivatives designed as efflux pump inhibitors: Molecular modeling and spectroscopic studies. *Molecules*, 26(8), 2374. <https://doi.org/10.3390/molecules26082374>
43. Ventola, C. L. (2015). The antibiotic resistance crisis: part 1: causes and threats. *Pharmacy and Therapeutics*, 40(4), 277–283.
44. Walther, D., et al. (2007). Structural basis for specificity in response regulator–DNA interactions. *Proceedings of the National Academy of Sciences*, 104(16), 7331–7336. <https://doi.org/10.1073/pnas.0702555104>
45. World Health Organization. (2021). Global antimicrobial resistance and use surveillance system (GLASS) report 2021. <https://www.who.int/publications/i/item/9789240027336>
46. Yao, X., et al. (2013). Central barrel interactions in TolC efflux channel function. *Biochemistry*, 52(17), 2966–2974. <https://doi.org/10.1021/bi4003937>
47. Yu, E. W., Aires, J. R., McDermott, G., & Nikaido, H. (2005). A periplasmic drug-binding site of the AcrB multidrug efflux pump: Crystallographic and site-directed mutagenesis study. *Journal of Bacteriology*, 187(19), 6804–6815. <https://doi.org/10.1128/JB.187.19.6804-6815.2005>
48. Yu, E. W., McDermott, G., Zgurskaya, H. I., Nikaido, H., & Koshland, D. E., Jr. (2003). Structural basis of multiple drug-binding capacity of the AcrB multidrug efflux pump. *Science*, 300(5621), 976–980. <https://doi.org/10.1126/science.1083134>
49. Zhou, L., Sreenivasan, A., Fong, S., & Calvey, E. (2006). Structural insights into the response regulator PhoP from *Mycobacterium tuberculosis*. *Journal of Molecular Biology*, 356(1), 121–129. <https://doi.org/10.1016/j.jmb.2005.10.033>